Available online at www.sciencedirect.com
ScienceDirect
Journal of the European Ceramic Society 28 (2008) 919–927
www.elsevier.com/locate/jeurceramsoc

Nanoreactor engineering and SPS densification of multimetal oxide ceramic nanopowders

Oleg Vasylkiv *, Hanna Borodianska, Yoshio Sakka

National Institute for Materials Science, 1-2-1, Sengen, Tsukuba, Ibaraki 305-0047, Japan

Available online 18 October 2007

Abstract

The concept of the *in situ* engineering of nanoreactors has been suggested and realized. Nanoreactors are morphologically homogeneous aggregates of synthesized complex intermediate metastable products. The thermo-activated processes of nucleation-growth of the final compositions were realized within the preliminary localized volume of each single nanoreactor, which provides the heredity of the final structure of the nanosize products. This new approach of multimetal oxide nanosize powder engineering allowed the prevention of the uncontrolled agglomeration and production of ceramic powders (8YSZ, CGO) consisting of ~45 nm nano-aggregates of ~7 nm crystallites with a remarkably homogeneous composition and uniform morphology. The advances from the introduction of the nanoblast calcination technique were also demonstrated. Finally, the SPS consolidation of nanosized aggregates of 8YSZ and CGO was analyzed. The 8YSZ ceramic with an average grain size of 90 nm and CGO nanoceramic with an extremely fine grain microstructure were obtained by low-temperature SPS under the ambient pressures of 100–150 MPa. The CGO ceramics with average grain sizes of 73, 32 and 18 nm were obtained by SPS at 1100, 1050 and 1000 °C, respectively.

Keywords: Powder-chemical preparation; Calcination; Nanocomposites; CeO_2; ZrO_2

1. Introduction

Multi-component ceramic nanosize powders enable quality improvement and differentiation of product characteristics at scales currently unachievable by commercially available micron- and submicron-size powders. The fabrication of nanopowders with a uniform morphology and precise stoichiometry is a key to realizing high-performance devices based on nanostructured metal oxide ceramics for a wide range of applications.[1–3]

Oxygen-ion conducting solid electrolytes have found wide applications in energy conversion, combustion control, chemical processing, and electrochemical cells for measuring the oxygen activities and thermodynamic data of solid, liquid and gaseous phases.

Y_2O_3-stabilized ZrO_2 (YSZ) is the most common electrolyte among the entire ZrO_2-based electrolytes used in solid oxide fuel cells (SOFC) and oxygen sensors because of its adequate ionic conductivity, stability in a dual environment (oxidizing and reducing) and durability against reaction by-products at the electrodes. Its ionic conductivity is consistently higher than 0.1 S/cm at 1000 °C, and the electronic conductivity is less than 10–4 S/cm over the entire oxygen potential region for the fuel cell operation.[5]

However, during the past decade, CeO_2-based materials have been intensively investigated as catalysts, structural and electronic promoters of heterogeneous catalytic reactions and oxygen-ion conducting solid electrolytes in electrochemical cells. For the last of these applications, the highest possible ionic conductivity of the solid electrolyte is required for device performance. At the temperatures of 700–800 °C, the rare-earth (RE)-doped ceria has a higher oxygen-ion conductivity than that of the yttria-stabilized zirconia.[10–12]

Ceramic nanopowders are usually synthesized by several aqueous-solution-based precipitation techniques.[1–19] Preparation techniques have included approaches based on sol–gel processing,[5–26] a reverse-micellar nanoreactor,[3,4] hydrothermal synthesis,[13–15] the sonochemically and/or microwave-assisted decomposition of various aqueous (or non-aqueous) precursor solutions,[15] salt-assisted aerosol decomposition and combustion synthesis.[16–17] However, due to the differences in the synthesis kinetic, high surface energy of the nanoparticles, and its chemical activity, hard agglomeration and the compositional inhomogeneity are the main problems encountered in

* Corresponding author. Tel.: +81 29 851 3354x8820; fax: +81 29 860 4706.
E-mail address: oleg.vasylkiv@nims.go.jp (O. Vasylkiv).

0955-2219/$ – see front matter © 2007 Elsevier Ltd. All rights reserved.
doi:10.1016/j.jeurceramsoc.2007.09.029

nanosynthesis.[1–26] One possibility of solving these problems[21] is an elaboration of the nanoparticles synthesis process inside the confined multifunctional microreactors. Such a microreactor is a polyelectrolyte capsule with controlled shell permeability and the possibility of shell engineering on the nanolevel, thus tailoring different functionalities. The advantages of such microreactors are absence of particle agglomeration (1), amorphous or metastable crystal phases (2), and unique composite inorganic/organic structures. However, the main disadvantage of such a methodology is an extremely low productivity of these kinds of microreactors.

The first aim of the present study was an establishing of a synthetic technique that will allow the development of thermo-activated synthesis processes of the final compositions within the preliminary localized volume of single nanoreactors. Based on our opinion, this would provide the heredity of the final structure and chemical homogenity of the nanosize products. The productivity of the produced methodology should be appropriate for the subsequent application of synthesized powders for the production of nanostructured dense ceramics.

In addition, for the thermal decomposition of preliminary engineered nanoreactors in this study, we employed the recently developed nano-explosive technique.[18,19] Explosions involve a rapid and violent oxidation reaction with a sudden release of mechanical and chemical energy in a violent manner, accompanied with the generation of a high temperature and the release of extremely hot gases. It causes pressure waves in the local medium in which it occurs.[21] Cyclotrimethylene trinitramine, used in this study, is an explosive material in its pure synthesized state, is a heterocycle and thus ring-shaped with the following structural formula: hexahydro-1,3,5-trinitro-1,3,5-triazine or $(CH_2\text{-}N\text{-}NO_2)_3$.[20] At room temperature, it is extremely stable, but partially soluble in ethanol. Its thermal decomposition starts at about 170 °C, melting at 204 °C, and it become explosive at 233 °C.[18–20]

The method we now describe still has no analogs, and after scaling up, promises to become a key technological solution for advanced nano-technologies. It allows overcoming the main drawbacks, that is, structural and compositional inhomogeneity,[1–3] of the numerous chemical methods of producing multi-component nanopowders—even those by combustion synthesis,[16,17] the method most closely related to ours. This is particularly important as agglomeration is considered to be a major hurdle in obtaining the full densification of nanometric powders produced by wet chemistry methods.

The last aim of the present study is to produce nanograined ceramics from preliminary engineered morphologically and compositionally homogeneous nanosize 8YSZ and CGO powders using a low-temperature spark plasma sintering (SPS) technique.

The SPS method has received much attention, because it sinters many materials at lower temperatures within few minutes. In the SPS method, the powder sample in a graphite die is pressed in a vacuum, and heated by a pulse current. The die is heated by the joule heat. It is said that the sintering proceeds very quickly because of the spark plasma caused by the large pulse current. Spark-plasma sintering, also known as electric-discharge sintering or Field-Assisted Sintering is a promising technique of powder consolidation. This approach involves the rapid heating of a powder by an electric current with the simultaneous application of an external pressure. Numerous experimental investigations point to the ability of SPS to render highly dense powder products with the potential of grain size retention. The latter ability is of significance for the consolidation of nanopowder materials, where the grain growth is one of the major problems.[22–27]

In this method, necks between powders are activated by spark plasma induced by a large pulse current. Diffusion mainly occurs only at the part that is needed for sintering. Diffusion at another part, which is a large fraction in the sample, is slow because the temperature is lower. Thus, it is expected that the change in the compositional distribution is small. This means that sintering with almost no change in the compositional distribution can be performed.[24–26] By SPS, a powder compact can be sintered at a lower temperature than that for conventional sintering. This should be attributed to the *in situ* particle surface activation and purification by the spark plasma generated during the process. Therefore, heat-transfer and mass-transfer between the particles can be instantaneously completed. Three factors that contribute to the fast densification process have been identified as: rapid heat transfer (1), the application of mechanical pressure (2), the use of fast heating and/or cooling rates (3).[25–27]

2. Experimental procedure

$ZrO(NO_3)_2{\cdot}nH_2O$ (99.9% pure and produced by Wako Pure Chemicals Co., Japan), and YCl_3 produced as described elsewhere[14] were weighed and dissolved in water at a total concentration of 0.1 M. The initial amount of zirconium and yttrium compounds varied according to the concentrations of both compounds in the resulting composites. The preparation conditions of the 8YSZ nanopowder were well described in earlier papers.[14,15] Urea (NH_2CONH_2 99% pure and produced by Wako Pure Chemicals Co., Japan) was used as a precipitation agent in the present study.

For the $Gd_{20}Ce_{80}O_{1.95}$ (CGO) synthesis, $CeCl_3{\cdot}7H_2O$, and $GdCl_3{\cdot}6H_2O$ (both 99.9% pure from Wako Pure Chemicals Co., Osaka, Japan) were weighed and separately dissolved in doubly distilled and deionized water at a concentration of 0.1 M. The initial amount of the cerium and gadolinium compounds varied according to the concentrations of both ceramic oxides in the resulting solid solution.

To produce intermediate nanoreactors, i.e. complex bi-metal aggregates, NH_2CONH_2 was dissolved in deionized water at the concentration of $2\,M/1-xM$ of $ZrO(NO_3)_2{\cdot}nH_2O$ or $CeCl_3{\cdot}7H_2O$ and xM $GdCl_3{\cdot}6H_2O$. Two jars with the total volume of the NH_2CONH_2 aqueous solution of 300 ml (200 ml for zirconium oxynitrate solution with 50 ml of yttrium chloride solution added for the 8YSZ preparation or cerium chloride, and 100 ml for the gadolinium chloride solutions) were prepared.

Both kinds of nanoreactors were synthesized as follows:

(1) To produce the matrix porous aggregates, nucleation of the zirconium and cerium oxide in the aqueous solution was

Table 1
The size distribution of the bi-component intermediate cerium–gadolinium compounds and three-component nanoreactors loaded with the $C_3H_6N_6O_6$, as synthesized, after multiple nanoblast calcinations at 450 °C with 30-min finalization holds

Composition	Engineered nanoreactors (nm)	Aggregate size distribution after nanoblast treatment (nm)	Aggregate size distribution after calcination at 450 °C (nm)	Primary crystallite size distribution (nm)
$Gd_{20}Ce_{80}O_{1.95}$ without $C_3H_6N_6O_6$	17–83	–	22–74	3–7
$Gd_{20}Ce_{80}O_{1.95}$ with $C_3H_6N_6O_6$	22–110	18–67	–	4–8

conducted by spraying 200 ml of a urea aqueous solution into the $ZrO(NO_3)_2{\cdot}nH_2O$ or cerium chloride aqueous solution. $CeCl_3{\cdot}7H_2O$ solution was heated to 80 °C with stirring at 1000 rpm and mixed under the prescribed conditions for 10 h. The gadolinium complex was nucleated by spraying the gadolinium chloride aqueous solution into a rapidly stirred (1600 rpm) suspension of the as-synthesized cerium oxide. Because of the existence of residual non-reacted urea, decomposition began immediately upon starting the gadolinium chloride solution spraying. After 30 min, 100 ml of the urea solution was added by spraying into the stock suspension. Subsequent stirring at 80 °C for five more hours was conducted to finalize the synthesis and homogenize the suspension. Finally, the product was washed with water followed by re-dispersion (according to Ref. 14) of the soft agglomerates of the cerium and gadolinium intermediate compounds in ethanol (C_2H_5OH, 99.5% reagent grade, Kanto Chemicals, Japan) using an ultrasonic horn (Model USP-600, Shimadzu, Kyoto, Japan).

For the zirconia synthesis, tock aqueous solutions of concentration 0.1 M of Zr^{4+} + 3 mol% of $2Y^{3+}$ were produced for the preparation of powder characterization samples and maintained by magnetic stirring at 20 °C (room temperature) for 24 h for the best homogenization. The 250 ml of mixed urea-containing sol in which the initial pH was ~1.2 after homogenization, was hydrothermally treated. Each sample was filled to 80 vol% in a 250 ml Teflon vessel held in an outer pressure vessel made of stainless steel. After the vessel had been sealed, it was heated to 155 °C for 50 h. Fifty hours is a total duration of the hydrothermal treatment. The urea decomposed into NH_3 and CO_2 through reaction with H_2O and the sol's pH changed to ~8.5. The homogeneous precipitate formed was hydrous yttria-doped ZrO_2, which crystallized under hydrothermal conditions.

(2) To produce cyclotrimethylene trinitramine ($C_3H_6N_6O_6$), hexamethylenetetramine was dissolved in deionized water at the concentration of 0.1 M. Concentrated (~93%) nitric acid (from Wako Pure Chemicals Co., Osaka, Japan) was added to the urotropin solution. Mixing urotropin with nitric acid causes the formation and precipitation of cyclotrimethylene trinitramine ($C_3H_6N_6O_6$).[18–20] Mixing the dissolved hexamethylenetetramine with diluted nitric acid causes the formation of well-dispersed nanoparticles of the $C_3H_6N_6O_6$ in the solvent.
(3) Nanoreactors were produced by dissolving the cyclotrimethylene trinitramine in ethanol with subsequent loading of the porous uniform matrix aggregates of the complex cerium–gadolinium intermediate compounds with the finest particles of $C_3H_6N_6O_6$. Subsequently, loaded with explosive compound nanoreactors were slowly dried in a drying oven at 70 °C and re-dispersed with no additional washing. The final multiple nano-explosive synthesis was conducted in the similar manner as previously described.[18,19]

A spark plasma sintering system (Sumitomo Coal Mining SPS system, Dr. Sinter Modal 1050, Japan) was used to prepare the SPS consolidated compacts. The powders were loaded into a graphite die (10 mm in diameter) and punch unit. In a typical densification experiment, 0.3–0.5 g of the ceramic nanopowders or pressed and subsequently CIPed in 400 MPa powder cylinders were loaded into the die which was then placed inside the SPS apparatus. All synthesized powders included in Table 1 were all characterized as having primary crystallite size below 10 nm.

A low pressure was initially applied. The vacuum level of the chamber was 4.5 Pa for the powder densification, and the applied compression was 25 MPa. The powder was first heated to 600 °C (the lowest controllable temperature of SPS) at the heating rate of 200 °C/min and then heated to the set temperature at vari-

Table 2
Characteristics of the 8YSZ and the CGO powders, SPS details, and properties of consolidated ceramics

Composition	Average aggregate size (nm)	Average primary crystallite size (nm)	Heating rate (°C/min)	Hold temperature during SPS (°C)	Relative density (%)	Average grain size (nm)
8YSZ	~90	~9	400	1250	>96.3	~1170
				1150	>98.9	~94
				1100	>89.2	~83
$Gd_{20}Ce_{80}O_{1.95}$	~70	~5	500	1100	>92.3	~176
				1050	>98.1	~123
$Gd_{20}Ce_{80}O_{1.95}$ nano-explosively calcined/deagglomerated	~45	~6	500	1100	>93.8	~73
				1050	>98.7	~32
				1000	>95.6	~18

ous heating rates in the starting current range of 600–1000 A as listed in Table 2. The corresponding voltage lies between 3.0 and 4.5 V, respectively. The electric current was periodically pulsed at 14 pulses/s (2 of 14 pulses off as a recovery time). The temperature was measured using a pyrometer placed in hole on the surface of the graphite die cylinder. The heating rates were 400 and 500 °C/min; the dwell time was 1 min. The final temperature after overshooting for 30–40 °C returned to the prescribed equilibrium value within the following 30 s.

After holding the powder samples (either just poured into the die or initially prepressed and CIPed) at the desired temperature in the range of 900–1250 °C, and pressure range of 30–150 MPa, the applied electric current was stopped, the pressure was released, and the sample was gradually cooled to 600 °C at the cooling rates of 10–100 °C/min and subsequently furnace cooled to room temperature.

The relative density of the gadolinia-doped ceria and 8YSZ ceramics were based on 7.15 g/cm^3 and 5.89 g/cm^3, respectively. The particle-size distribution was analyzed by the dynamic light scattering method (DLS) using a laser particle-size analyzer (Model LSPZ-100, Otsuka Electronics, Osaka, Japan). A very small amount of each powder (∼5 mg) was dispersed in the distilled water for the analysis. Observation via TEM (Model JEM-2100-F, JEOL, Tokyo, Japan) operated at 200 kV was used to determine the nanoreactors and final powders morphologies. Phase identification of the powders and distribution of the components into each aggregate were determined by a nano-area energy dispersion X-ray spectroscopy analyzer (TEM-EDX).

For analyzing the sintered ceramic, a Hitachi FESEM S-4800 operated at 5 kV and 200 nA was used. No conductive coating was applied on the fracture surface. The average grain size was determined from high-resolution SEM images of the fracture surfaces. The determination of the grain size in the densified nanometric oxides in a range below 50 nm is particularly challenging. Most of the traditional and well-established ceramographic techniques cannot be used in this range. It is already known[27] that thermal etching of polished surfaces cannot be performed on these samples as the high temperatures required by this process can produce a significant alteration of the grain size. Moreover, it is also recognized that polishing can produce a significant stress-induced peak broadening in zirconia and other ceramics.[27] In samples with grain sizes below 50 nm, the stress cannot be annealed out without producing a modification in the grain size.

3. Results and discussion

3.1. Synthesis of 8YSZ dense aggregates via preliminary engineered nanoreactors

After hydrothermal treated at 155 °C for 5 h, the aqueous solution of yttrium–zirconium intermediate complex was rapidly cooled and removed from the Teflon vessel. The ultrasonic dispersion for 1 min was applied to destroy the initial soft contacts between the as-nucleated and clustered yttrium–zirconium compounds. The produced extremely stable (no precipitation for 100 h was detected at pH 10) aqueous suspension was then poured into a Teflon vessel again and mounted on the magnetic stirrer. Suspension was than intensively stirred for next 45 h at 155 °C. After cooling and subsequent washing, the produced uniformly aggregated 8 mol% yttria 92 mol% zirconia hydrous particles where analyzed by TEM and a nano-area energy dispersion X-ray spectroscopy analyzer (TEM EDX) which confirmed the morphological and compositional homogeneity of the as-synthesized yttrium–zirconium intermediate nanoreactors. The uniformity of morphology of the hydrous yttria-doped zirconia aggregates that consist of very fine primary particles is shown on Fig. 1. The TEM-EDX mapping image of the hydrothermally synthesized 8YSZ intermediate nanoreactors (Fig. 2) shows the remarkably uniform distribution of yttrium within the zirconium matrix aggregates.

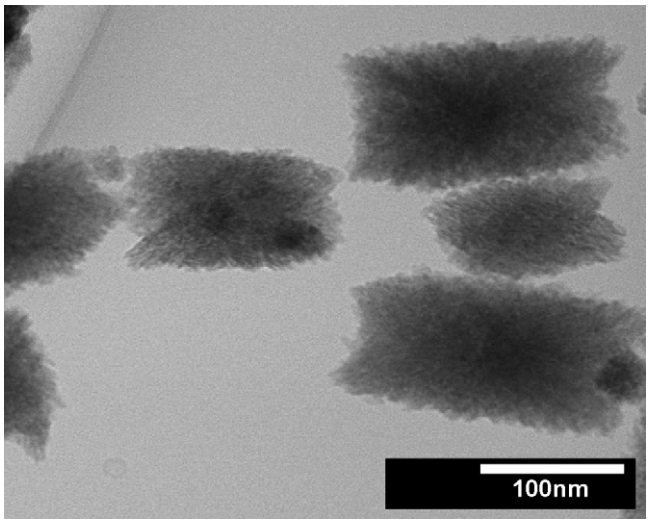

Fig. 1. Engineered nanoreactors of yttria–zirconia compounds.

The following calcination at 600 °C for 30 min resulted in uniformly shaped dense aggregates of fully stabilized cubic zirconia. A TEM micrograph of the 8 mol% yttria-stabilized zirconia (8Y-ZP) nanopowder is shown in Fig. 3. The primary crystallites with an average size of ∼9 nm are aggregated into secondary nano-aggregates with a mean aggregate size of 30–110 nm. The satisfactory heredity of the final nano-aggregates morphology can be observed in Figs. 1 and 3. Such a powder morphology was found to be extremely important for the preparation of uniform green samples which are only acceptable for subsequent low-temperature sintering.

3.2. Synthesis of cerium–gadolinium oxide nanopowders through preliminary engineered nanoreactors

The primary particles of the as-synthesized ceria assembled into fine aggregates covered by direct spraying with the as-synthesized clusters of the gadolinium intermediate complex that formed the matrix bi-metal nanoreactors.

Table 1 shows the size distribution for bi-component intermediate cerium–gadolinium compounds and three-component nanoreactors loaded with $C_3H_6N_6O_6$, as synthesized, after multiple nanoblast calcinations at 450 °C with 30-min finalization holds. This table includes particle size data for the as-synthesized

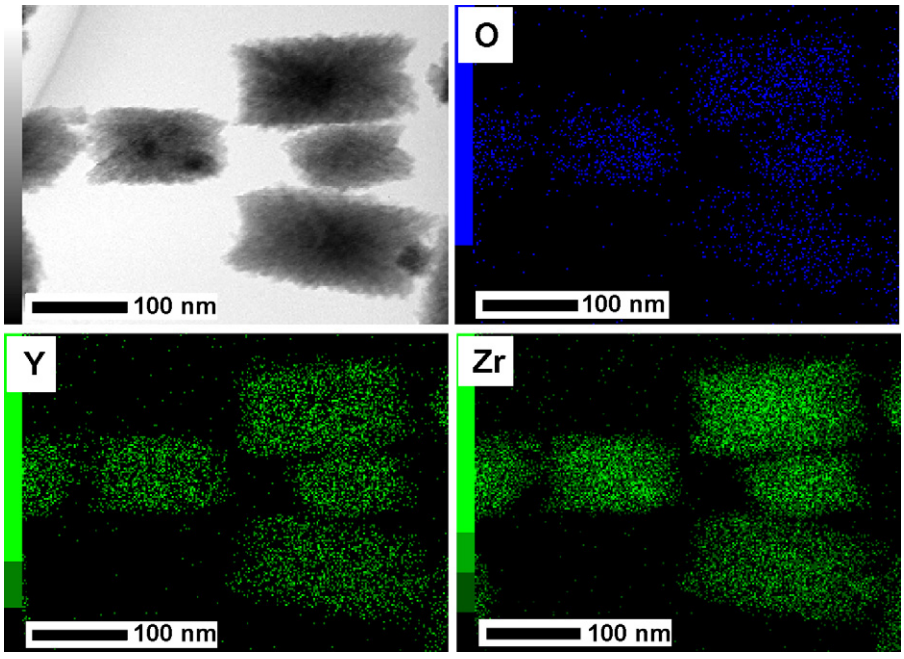

Fig. 2. TEM EDX maping of yttria–zirconia intermediate nanoreactors.

nanoreactors, particle size distribution after the calcinations (in case of thermal decomposition of engineered bi-component nanoreactors) and, finally, characteristics of the powders produced by multiple nanoblast calcination/deagglomeration from nanoreactors loaded with cyclotrimethylene trinitramine. In both cases, the temperature of the calcination was 450 °C with 30-min holds.

Prior to the calcinations both of the well-dried powders that were composed of the bi-metal complex intermediate aggregates and the same aggregates, but additionally loaded with $C_3H_6N_6O_6$ that were briquetted by uniaxial pressing at 4 MPa and separately filled into an alumina container for further thermal treatment. In the case of applying the nanoblast technique, prevention of the undesirable ignition of the $C_3H_6N_6O_6$[18–20] was extremely important. For this reason ultra-rapid heating of the loaded nanoreactors through the thermal detonation temperature (~230 °C for cyclotrimethylene trinitramine) was applied. This thermal detonation temperature, i.e. the temperature at which spontaneous multiple ruptures of the $N–NO_2$ bonds occur, strongly depends on the heating rate which may vary from 220 to 360 °C. Extremely rapid detonation (10^{-8} s/g) of $C_3H_6N_6O_6$ separated into the porous matrix ceramic aggregates (i.e. nanoreactors) forms gaseous products with a temperature of 2500 °C compressed into localized volumes equaling the initial volumes of each explosive particle. Multiple nanoblasts occur within the volume of the three-component nanoreactors. The instantaneous power of each blast is 500 MW/g.[20] The multiplied local impacts of the nanoblast waves lead to the fragmentation of the surrounding matter, i.e. deagglomeration of the powder. The rapid evolution of a large volume of extremely hot gaseous products dissipates the heat of the process and limits the temperature increase to localized areas. The last circumstance reduces the possibility of premature local partial sintering among the neighboring crystallites resulting in a non-agglomerated product. In addition, due to the short-term high temperature generation, which enhanced the solubility of the components nanosize solid solution of the dopant gadolinium oxide into the matrix cerium oxide, was synthesized. Utilizing the described technique, non-agglomerated cerium–gadolinium oxide (CGO) powder (Fig. 4) with an average primary crystallite size range of 3–9 nm, and an aggregate size of ~45 nm (see Table 2) was produced.

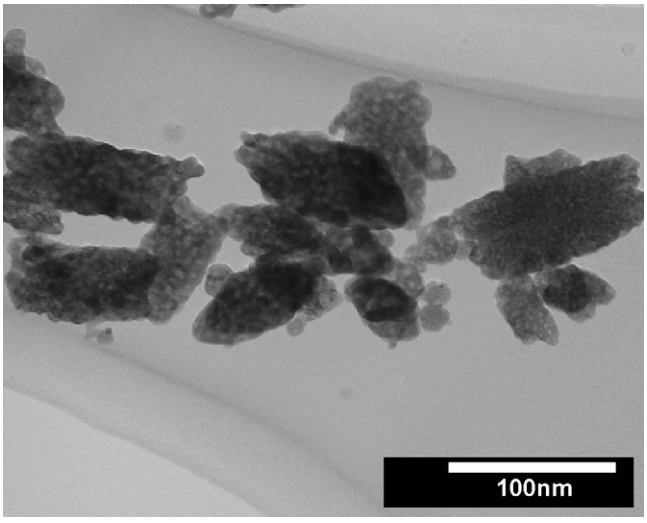

Fig. 3. The 8YSZ engineered nano-aggregates.

3.3. SPS densification of produced 8YSZ and CGO nanopowders

Finally, the consolidation of the powder samples of 8YSZ and CGO by spark plasma sintering (with and without preliminary

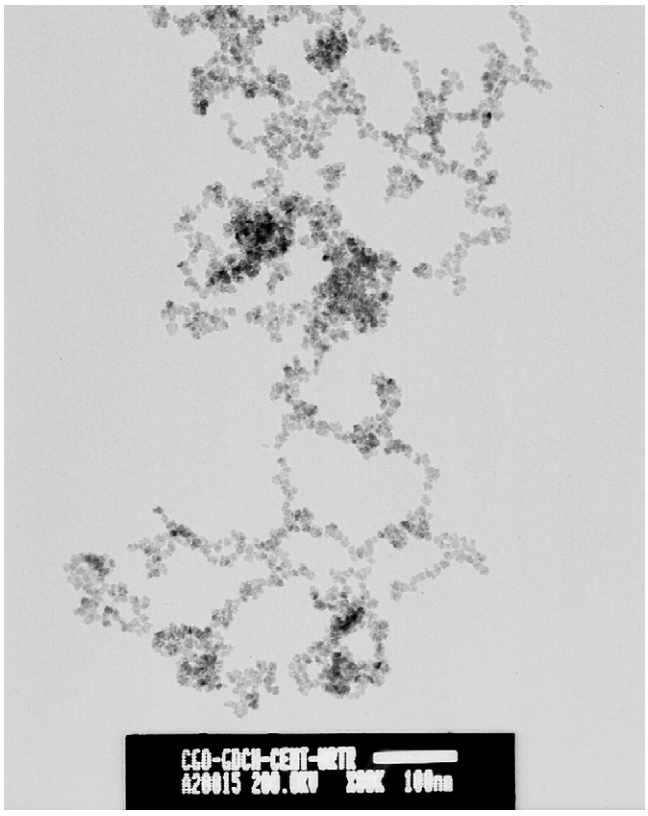

Fig. 4. The CGO non-agglomerated nanoparticles explosively calcined from the preliminary engineered nanoreactors impregnated with the $C_3H_6N_6O_6$.

CIPing) under different temperature/time conditions, pressures and starting current was analyzed with aim of obtaining high dense nanograined ceramics.

Anselmi-Tamburini et al.[27] showed the possibility of obtaining dense zirconia and ceria ceramics with grain sizes approaching 10 nm using a high-pressure modification of the field activated sintering (spark plasma sintering). Pressures up to 1 GPa and sintering times of 5 min have been used by them. In their case, the densification has been performed at temperatures as low as 930 °C for the fully stabilized zirconia, 815 °C for the samaria-doped ceria, and 675 °C for the pure ceria. Relative densities greater than 98% were achieved for all the materials. The authors claimed that their method overcomes the deleterious effect of powder agglomeration, producing fine grain sizes for these ceramics in bulk form. In order to reach very high pressures, the authors developed a double acting die to achieve pressures as high as 1 GPa on a sample 5 mm in diameter and 1–3 mm thick, while maintaining the ability of fast sintering cycles. Their device was composed of an external graphite die, very similar in shape to a traditional SPS die. Two protective discs of pure, fully dense tungsten carbide are placed at the end of each plunger. The internal, smaller die also has a graphite body, but with plungers made out of silicon carbide. It was shown that the combination of fast heating rate and high pressure produces a marked reduction in the sintering temperature for the SPS densification of nanometric cubic zirconia. The reported[27] temperature required to reach 95% of the theoretical density for 8YSZ nanoceramic remarkably decreases with pressure and nearly fully dense samples were shown to be obtained in 5 min at temperatures even below 900 °C. To attain such a result, extremely high pressures even approaching 1 GPa were employed.[27] This reported remarkable temperature lowering is for several hundred degrees below the typical sintering temperatures (1300–1500 °C) required to obtain the full densification of zirconia (YSZ) using traditional pressureless sintering or hot-pressing. Both traditional methods also require long sintering times. The decrease in the sintering temperature and time produces a marked decrease in grain growth.[27] The authors noted that in their case, the starting powders were heavily agglomerated. However, their densification procedure has been effective in the elimination of the mesoporosity, which is associated with the agglomeration of nanopowders.

In the current study, the maximum applied pressure was only 150 MPa. This allowed us to use the ordinary high-strength graphite die with no additional modifications. However, as distinct from the study of Anselmi-Tamburini et al.,[27] the characteristics of the starting powders for current investigation were thoroughly controlled. The initial nanopowders of 8YSZ and CGO were synthesized by a nanoreactor engineering technique with the aim to attain the highest possible compliance between the primary crystallite size, powder morphology (i.e. aggregate size distribution and its morphological homogeneity) and minimization of the residual agglomeration.

The characteristics of the ceramics consolidated using the SPS technique are listed in Table 2. This table shows the average aggregate and crystallite sizes of the 8YSZ and CGO ceramic nanopowders obtained by the techniques described in Sections 3.1 and 3.2 of the current study.

The SEM micrograph of the 8YSZ ceramic consolidated by SPS at 1250 °C for 5 min is shown on Fig. 5. Such coarse-grained ceramic was obtained due to the use of the 8YSZ powder sample with no preliminary cold isostatic pressing, which reduced the possibility of the SPS temperature lowering. Pretreatment of the green samples by CIP at 400 MPa allowed a significant reduction of the SPS consolidation temperatures. The SEM micrograph of the 8YSZ ceramic consolidated by SPS at 1150 °C for 5 min

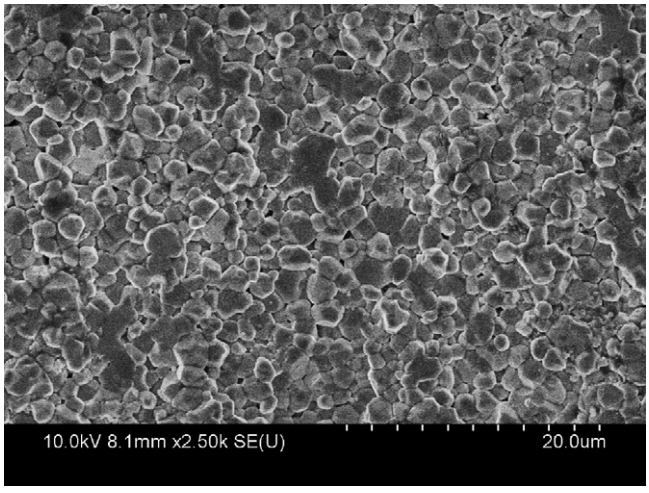

Fig. 5. The 8YSZ ceramic consolidated by the SPS with 5-min holds at 1250 °C.

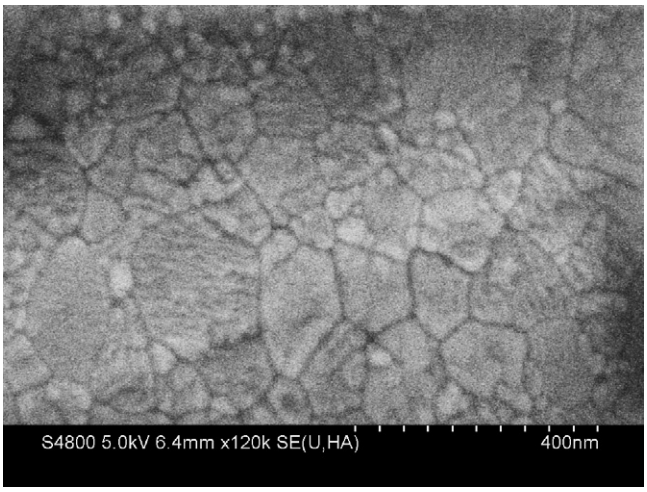

Fig. 6. The 8YSZ with 1 mass% of the Al_2O_3 ceramic consolidated by the SPS with 5-min holds at 1150 °C.

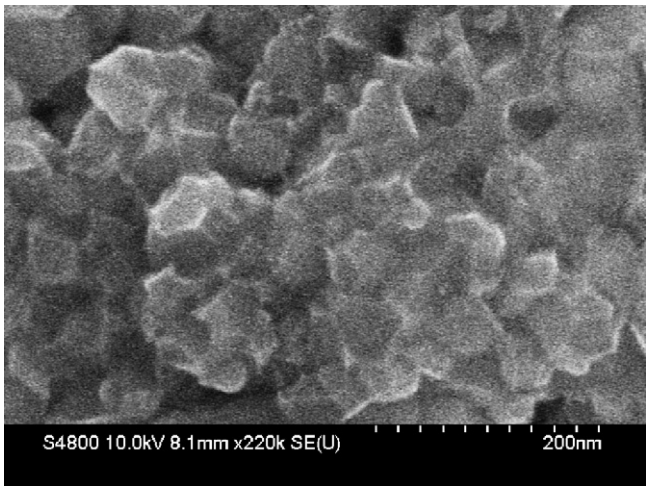

Fig. 7. The CGO ceramic consolidated by the SPS with 5-min holds at 1100 °C.

is shown in Fig. 6. To enhance sinterability and to attain the high density by SPS at 1150 °C, 1 mass% of the γ-Al_2O_3 was colloidally added to the 8YSZ prior to consolidation.[28,29]

Comparing the average grain size of the 8YSZ ceramic after SPS consolidation with the initial average aggregate size, it is evident that the grain growth is very limited. Actually, we can conclude that only intra-aggregate recrystallization occurs and each aggregate became a single grain (See Table 2 and Fig. 6).

During the sintering process, the pressure increases from 30 MPa while reaching 100 MPa at a maximum temperature with a subsequent gradual rise to 150 MPa during the 5-min holds. The pressure maximum of 150 MPa was applied at the punch unit for all samples either preCIPed or just poured powder samples. The electric current employed was typically 600–900 A at 600 °C that corresponds to 400–600 A at the holding temperatures. The last condition means that the current gradually decreases with the increasing temperature and sample density.

As shown in Table 2, the relative densities of the 8YSZ ceramic samples cold isostatically pressed and sintered at 1100 and 1150 °C (both heated to the hold temperature at 400 °C/min) were >89.2% and >98.9% with an average grain size of 83 nm and 90 nm, respectively.

As shown in Table 2, the relative densities of the CGO ceramic samples cold isostatically pressed from the $Gd_{20}Ce_{80}O_{1.95}$ powder produced with no application of multiple nano-explosions and sintered at 1100 and 1050 °C (heated to the holding temperatures at 500 °C/min) were >92.3% and >98.1% with an average grain size of 176 nm and 123 nm, respectively. Such a relatively fine grain size distribution well corresponds with the average aggregate size of the initial powder. In addition, the lower relative density at the higher hold temperatures well corresponds to the concurrence between the intra-aggregate and inter-aggregate densifications at the different SPS regimes. It is possible to conclude that due to rapid intra-aggregate densification a residual inter-grain porosity exists. In the case of lowering the hold temperatures, rearrangement of the primary crystallites into aggregates, and cross-aggregate rearrangement became slower and balanced, and total densification was mostly determines by the applied external pressure. When excluding the influence of agglomeration (due to initial engineering of morphologically homogeneous nano-aggregates) on the densification, plastic or even superplastic deformation should become of significant importance. This would support a densification mechanism based on grain boundary sliding and grain boundary rotation. That is why the pressure became of great importance during the isothermal stage of SPS through rearrangement of the crystallites and densification through plastic or superplastic deformation.

The SEM micrograph of the CGO ceramic consolidated by SPS at 1100 °C for 5 min is shown on Fig. 7. This nanograined ceramic was obtained because of using the $Gd_{20}Ce_{80}O_{1.95}$ sample CIPed from the nanosize powder (Fig. 4) produced by a nanoblast technique from engineered nanoreactors impregnated with $C_3H_6N_6O_6$. The relative density of this sample was >93.8% and average grain size was ∼73 nm. Similar to the consolidation of the 8YSZ ceramic, pretreatment by CIP at 400 MPa allowed a significant reduction of the SPS consolidation temperatures and increased relative density of the sintered ceramic. The SEM micrographs of the CGO ceramics consolidated by

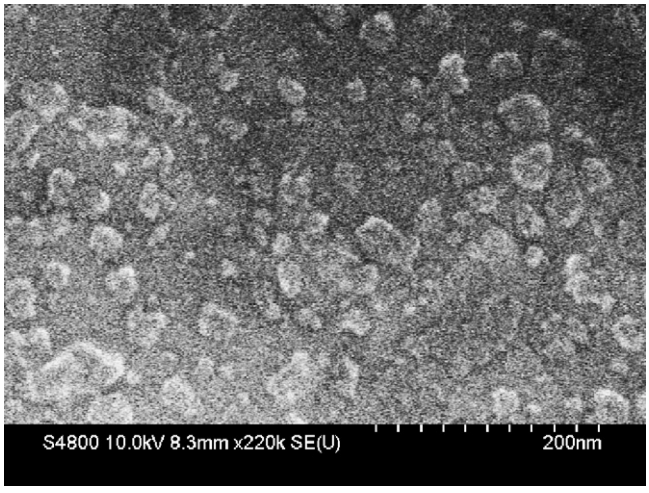

Fig. 8. The CGO ceramic consolidated by the SPS with 5-min holds at 1050 °C.

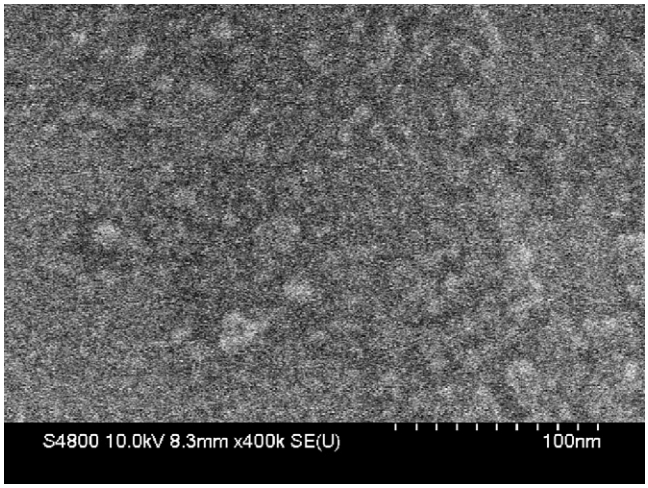

Fig. 9. The CGO ceramic consolidated by the SPS with 5-min holds at 1000 °C.

SPS at 1050 and 1000 °C for 5 min are shown in Figs. 8 and 9, respectively. The extremely fine-grained high dense nanoceramics were obtained by the SPS with 5-min holds at both temperatures (Table 2).

Similar to the SPS of cubic zirconia, a 100 MPa pressure was applied during heating at both hold temperatures. At the maximum temperature the pressure was gradually increased to 150 MPa during the final 5-min holds. As shown in Table 2, the relative densities of the CGO ceramic samples cold isostaticaly pressed and sintered at 1050 and 1000 °C (both heated to the hold temperature at 500 °C/min) were >98.7% and >95.6% with a remarkable fine average grain size of 32 and 18 nm, respectively.

For all the above conditions, the sintering temperatures are several hundred degrees lower then the temperatures used in conventional sintering methods. Very limited grain growth was evident. The morphological homogeneity of the starting powders for both 8YSZ and CGO plays a governing role in the success of the low-temperature SPS consolidation. The second significant role is use to be the applied pressure. As we already claimed above, the applied pressure plays its role through rearrangement of the crystallites through plastic (even superplastic) deformation especially during the last isothermal stage of the SPS consolidation.

4. Conclusions

The concept of the *in situ* engineering of nanoreactors, morphologically homogeneous aggregates of synthesized intermediate metastable products has been realized. The thermo-activated processes of nucleation-growth of the final compositions were realized within the preliminary localized volume of each single nanoreactor, which provides the heredity of the final structure of the nanosize products. This new approach of multimetal oxide nanosize powders engineering allowed the production of 8YSZ and CGO powders consisting of ∼45 nm nano-aggregates with a remarkably homogeneous morphology.

The 8YSZ ceramic with average grain size of 90 nm and the CGO nanoceramic with an extremely fine grain microstructure were consolidated by low-temperature SPS under ambient pressures of 100–150 MPa. The CGO nanoceramics with an average grain size of 73, 32 and 18 nm were obtained by SPS at 1100, 1050 and 1000 °C, respectively. Under these conditions, the sintering temperatures are much lower then the temperatures used in conventional sintering methods. Very limited grain growth was also evident. In addition, the significant role of sophisticatedly applied, unusually high pressure on the particle rearrangement through plastic or superplastic deformation was successfully demonstrated.

Such an accomplishment of our investigation opens the door to future investigations of the properties of bulk nanoceramics with such fine grain sizes that mesoscopic effects are anticipated.

References

1. Gleiter, H., Nanocrystalline materials: basic concept and microstructure. *Acta Mater.*, 2000, **48**, 1–29.
2. Tjong, S. and Chen, H., Nanocrystalline materials and coatings. *Mater. Sci. Eng. R*, 2004, **45**, 1–88.
3. Johnston, K. and Shah, P., Making nanoscale materials with supercritical fluids. *Science*, 2004, **303**, 482–483.
4. Pileni, M.-P., The role of soft colloidal templates in controlling the size and shape of inorganic nanocrystals. *Nat. Mater.*, 2003, **2**, 145–150.
5. Millman, J., Bhatt, K., Prevo, B. and Velev, O., Anisotropic particle synthesis in dielectrophoretically controlled microdroplet reactors. *Nat. Mater.*, 2005, **4**, 98–102.
6. Lee, J.-S. and Choi, S.-C., Crystallization behavior of nano-ceria powders by hydrothermal synthesis using a mixture of H_2O_2 and NH_4OH. *Mater. Lett.*, 2004, **58**, 390–393.
7. Vasylkiv, O. and Sakka, Y., Synthesis and sintering of zirconia nanopowder by non-isothermal decomposition from hydroxide. *J. Ceram. Soc. Jpn.*, 2001, **109**, 500–505.
8. Vasylkiv, O. and Sakka, Y., Non-isothermal synthesis of yttria-stabilized zirconia nanopowder through oxalate processing. I. Characteristics of (Y–Zr) oxalate synthesis and its decomposition. *J. Am. Ceram. Soc.*, 2000, **83**, 2196–2202.
9. Vasylkiv, O., Sakka, Y. and Borodians'ka, H., Non-isothermal synthesis of yttria-stabilized zirconia nanopowder through oxalate processing. I. Morphology manipulation. *J. Am. Ceram. Soc.*, 2001, **84**, 2484–2488.
10. Tianshu, Z., Hing, P., Huang, H. and Kilner, J., Ionic conductivity in the CeO_2–Gd_2O_3 system ($0.05 \leq Gd/Ce \leq 0.4$) prepared by oxalate co-precipitation. *Solid State Ionics*, 2002, **148**, 567–573.
11. Li, J.-G., Ikegami, T., Wang, Y. and Mori, T., $Ce_{1-x}Y_xO_{2-x/2}$ ($0 \leq x \leq 0.35$) oxides via carbonate precipitation: synthesis and characterization. *Solid State Chem.*, 2002, **168**, 52–59.
12. Zhang, T., Ma, J., Kong, L., Hing, P. and Kilner, J., Preparation and mechanical properties of dense $Ce_{0.8}Gd_{0.2}O_{2-\delta}$ ceramics. *Solid State Ionics*, 2004, **167**, 191–196.
13. Vasylkiv, O., Kolodiazhni, T., Sakka, Y. and Skorokhod, V., Synthesis and characterization of nanosize ceria-gadolinia powders. *J. Ceram. Soc. Jpn.*, 2005, **113**, 101–106.
14. Vasylkiv, O. and Sakka, Y., Synthesis and colloidal processing of zirconia nanopowder. *J. Am. Ceram. Soc.*, 2001, **84**, 2489–2494.
15. Vasylkiv, O., Sakka, Y., Maeda, Y. and Skorokhod, V., Nano-engineering of zirconia-noble metals composites. *J. Eur. Ceram. Soc.*, 2004, **24**, 469–473.
16. Ulrich, G., Flame synthesis of fine particles. *Chem. Eng. News*, 1998, **62**, 22–29.
17. Pratsinis, S., Flame aerosol synthesis of ceramic powders. *Prog. Energy Combust. Sci.*, 1998, **24**, 197–219.
18. Vasylkiv, O. and Sakka, Y., Nanoexplosion synthesis of multimetal oxide ceramic nanopowders. *Nano Lett.*, 2005, **5**, 2598–2604.
19. Vasylkiv, O., Sakka, Y. and Skorokhod, V. V., Nano-blast synthesis of nanosize CeO_2-Gd_2O_3 powders. *J. Am. Ceram. Soc.*, 2006, **89**, 1822–1826.

20. Kuklja, M., Thermal decomposition of solid cyclotrimethylene trinitramine. *J. Phys. Chem. B*, 2001, **105**, 10159–10162.
21. Shchukin, D. and Sukhorukov, G., Nanoparticle synthesis in engineered organic nanoscale reactors. *Adv. Mater.*, 2004, **16**, 671–682.
22. Angerer, P., Yu, L. G., Khor, K. A. and Krumpel, G., Spark-plasma-sintering (SPS) of nanostructured and submicron titanium oxide powders. *Mater. Sci. Eng. A*, 2004, **381**, 16–19.
23. Olevsky, E. and Froyen, L., Constitutive modeling of spark-plasma sintering of conductive materials. *Scripta Mater.*, 2006, **55**, 1175–1178.
24. Kakegawa, K., Uekawa, N., Wu, Y. J. and Sasaki, Y., Change in the compositional distribution in perovskite solid solutions during the sintering by SPS. *Mater. Sci. Eng. B*, 2003, **99**, 11–14.
25. Khor, K. A., Chen, X. J., Chan, S. H. and Yu, L. G., Microstructure-property modifications in plasma sprayed 20 wt.% yttria stabilized zirconia electrolyte by spark plasma sintering (SPS) technique. *Mater. Sci. Eng. A*, 2004, **366**, 120–126.
26. Chen, X. J., Khor, K. A., Chan, S. H. and Yu, L. G., Overcoming the effect of contaminant in solid oxide fuel cell (SOFC) electrolyte: spark plasma sintering (SPS) of 0.5 wt.% silica-doped yttria-stabilized zirconia (YSZ). *Mater. Sci. Eng. A*, 2004, **374**, 64–71.
27. Anselmi-Tamburini, U., Garay, J. and Munir, Z., Fast low-temperature consolidation of bulk nanometric ceramic materials. *Scripta Mater.*, 2006, **54**, 823–828.
28. Vasylkiv, O., Sakka, Y. and Skorokhod, V. V., Hardness and fracture toughness of alumina-doped tetragonal zirconia with different yttria contents. *Mater. Transac. JIM.*, 2003, **44**, 2235–2238.
29. Vasylkiv, O., Sakka, Y. and Skorokhod, V. V., Low-temperature processing and mechanical properties of zirconia and zirconia–alumina nano-ceramics. *J. Am. Ceram. Soc.*, 2003, **86**, 299–304.